

D. WEIDMANN<sup>1,✉,\*</sup>  
F.K. TITTEL<sup>1</sup>  
T. AELLEN<sup>2</sup>  
M. BECK<sup>2</sup>  
D. HOFSTETTER<sup>2</sup>  
J. FAIST<sup>2</sup>  
S. BLASER<sup>3</sup>

## Mid-infrared trace-gas sensing with a quasi-continuous-wave Peltier-cooled distributed feedback quantum cascade laser

<sup>1</sup> Rice Quantum Institute, Rice University, 6100 Main Street, Houston, TX, USA

<sup>2</sup> Université de Neuchâtel, Rue A.L. Breguet 1, 2000 Neuchâtel, Switzerland

<sup>3</sup> Alpes Lasers SA, 1–3 Max.-de-Meuron, CP 1766, 2000 Neuchâtel, Switzerland

Received: 18 June 2004/Revised version: 4 August 2004

Published online: 29 September 2004 • © Springer-Verlag 2004

**ABSTRACT** A recently developed distributed feedback quantum cascade laser (QCL) capable of thermoelectric-cooled (TEC) continuous-wave (cw) operation and emitting at  $\sim 9 \mu\text{m}$  is used to perform laser chemical sensing by tunable infrared spectroscopy. A quasi-continuous-wave mode of operation relying on long current pulses ( $\sim 5 \text{ Hz}$ ,  $\sim 50\%$  duty cycle) is utilized rather than pure cw operation in order to extend the continuous frequency tuning range of the quantum cascade laser. Sulfur dioxide and ammonia were selected as convenient target molecules to evaluate the performance of the cw TEC QCL based sensor. Direct absorption spectroscopy and wavelength-modulation spectroscopy were performed to demonstrate chemical sensing applications with this novel type of quantum cascade laser. For ammonia detection, a 18-ppm noise-equivalent sensitivity ( $1 \sigma$ ) was achieved for a 1-m absorption path length and a 25-ms data-acquisition time using direct absorption spectroscopy. The use of second-harmonic-detection wavelength-modulation spectroscopy instead of direct absorption increased the sensitivity by a factor of three, achieving a normalized noise-equivalent sensitivity of  $82 \text{ ppb Hz}^{-1/2}$  for a 1-m absorption path length, which corresponds to  $2 \times 10^{-7} \text{ cm}^{-1} \text{ Hz}^{-1/2}$ .

PACS 42.55.Px; 42.62.Fi; 07.88.+y

### 1 Introduction

Tunable laser spectroscopy has proved to be a technique well suited for achieving gas-phase concentration measurements from the ppm level to the low ppb range. Compact laser sources that emit in the mid infrared, where most molecules exhibit fundamental and therefore strong absorption ro-vibrational bands, are particularly useful. Among the available tunable laser sources, distributed feedback (DFB) quantum cascade lasers (QCLs) offer several unique advantages for the design of compact field-deployable optical sensors, such as high output power, narrow laser line width, compactness, robustness, single-mode operation, and

thermoelectric-cooled (TEC) operation in a pulsed mode regime [1, 2].

Until now, due to the relatively short upper-state lifetime of the involved intersubband transitions occurring in QCLs, their high operating voltage of nearly 10 V, and the associated large heat dissipation within the active zone, single-frequency operation has been achieved only in a pulsed mode at room temperature. Pulsed QCL operation suffers from three drawbacks: (1) due to thermal chirping, even a  $\sim 10$ -ns pulse generates typical QCL line widths of  $\sim 200$ – $300 \text{ MHz}$ , which is substantially larger than the Fourier-transform limit; (2) the main sensitivity limitation of a pulsed DFB QCL based spectrometer arises from the pulse to pulse intensity fluctuations that require the use of an additional reference beam for normalization [3, 4]; and (3) the generation of nanosecond current pulses requires high-speed driving electronics and detectors as well as fast data acquisition. To overcome these drawbacks, considerable effort has been made towards achieving a DFB QCL that is able to operate in a continuous-wave (cw) mode at room temperature.

A first device, employing high-reflection-coated facets and operating up to 312 K, was demonstrated by Beck et al. [5]. This device had no DFB structure and operated in single mode, most likely because of a small defect in the laser cavity. Recently, high-power cw QCLs have been developed to operate at  $4.3$ – $6 \mu\text{m}$  at power levels up to 600 mW [6], but as Fabry–Pérot devices these lasers exhibit multimode emission. More recently, new devices emitting at  $\sim 9$  and  $5.4 \mu\text{m}$  with an embedded DFB structure have been developed [7, 8]. Such single-frequency DFB QCLs are able to operate in a cw mode at temperatures achievable by thermoelectric cooling.

In this paper we report the first spectroscopic application using such a cw TEC DFB QCL at  $9 \mu\text{m}$  with an output power of  $\sim 2 \text{ mW}$  at  $-40^\circ\text{C}$ . First, the QCL was characterized and an optimum mode of operation for gas sensing was determined. The QCL line width and the noise sources limiting detection sensitivity were investigated. Sulfur dioxide ( $\text{SO}_2$ ) direct absorption spectroscopy was performed for laser characterization. The sensor was subsequently used for the monitoring of ammonia ( $\text{NH}_3$ ), using both direct absorption spectroscopy and wavelength-modulation spectroscopy (WMS) with detection at the second harmonic.

✉ Fax: +1-713-348-5686, E-mail: d.weidmann@rl.ac.uk

\*Present address: Space Science and Technology Department, CCLRC Rutherford Appleton Laboratory, Chilton, Didcot, Oxfordshire, OX11 0QX, UK

## 2 Target molecules for gas monitoring

The QCL characterization began with a determination of the available wavelength tuning range for cw operation by means of a  $0.125\text{-cm}^{-1}$  resolution Fourier-transform spectrometer. These data have been previously presented in [7]. With a cw excitation current set to 680 mA, the device exhibited a frequency range from  $1113$  to  $1116\text{ cm}^{-1}$  by varying the temperature from  $-30$  to  $-70\text{ }^{\circ}\text{C}$ . A survey based on HITRAN 2000 [9] data within the  $1110\text{--}1115\text{ cm}^{-1}$  spectral window provided the potential target molecules accessible with the available device.

Among the molecules with the most intense ro-vibrational transitions in the QCL-accessible spectral window,  $\text{NH}_3$  and  $\text{SO}_2$  were selected to perform the sensor-evaluation study. The strong  $\text{NH}_3$  and  $\text{SO}_2$  spectral lines in the window belong to the  $\nu_2$  and  $\nu_1$  fundamental bands, respectively. Both of these trace gases are relevant in atmospheric chemistry.  $\text{NH}_3$  is the third most abundant nitrogen compound in the atmosphere and promotes the formation of ammonium aerosols. The emissions are mainly agricultural.  $\text{NH}_3$  is also a toxic industrial chemical.  $\text{SO}_2$ , which is released by fossil-fuel combustion related to human activity (and also by volcanoes in smaller amounts) is responsible for acid rains and promotes the formation of sulfate aerosols [10].

## 3 Description of gas-sensor architecture

The direct absorption spectrometer configuration shown in Fig. 1 was used in this study. The QCL is enclosed in a dry nitrogen atmosphere to prevent moisture deposition on the laser chip. The QCL housing base is a cold plate that allows circulation of pre-cooled water to enhance heat extraction from the TE cooler that regulates the QCL temperature. With the laser turned off, the lowest temperature achieved is  $-50\text{ }^{\circ}\text{C}$ . The laser is driven by a custom-built battery-based current source, which supplies up to 1.5 A with the high compliance voltage required by the cw QCL ( $\sim 11\text{ V}$ ). The QCL excitation source has two external modulation inputs as well as an internal function generator for the modulation of the QCL wavelength.

The infrared (IR) radiation from the QCL is collimated by an AR-coated  $f/0.5$  aspheric ZnSe lens and then passes through a 53.34-cm-long single-path absorption cell equipped with Brewster-angled ZnSe windows. The cell is connected to a gas-flow system with a controller for monitoring and adjusting the pressure. The beam exiting the cell is focused on to a  $1\text{-mm}^2$  HgCdTe detector by a 75-mm  $90^{\circ}$  off-axis parabolic mirror. The detector used is a liquid nitrogen cooled HgCdTe photodiode with a built-in pre-amplifier (Kolmar

model KMPV10-1-J1). This detector is in fact too sensitive for the available QCL laser output power and a TEC infrared detector would have been more appropriate. Therefore, it was necessary to attenuate the mid-IR probe beam in order to avoid the non-linear region of the detector response curve and saturation of the detector output. The attenuation was conveniently performed by rotating the absorption cell along the optical axis. In this manner, the Brewster-angled windows act as a polarizing analyzer for the transmitted QCL beam. The detected signals are acquired by a National Instrument PCMCIA card (model DAQCard-AI-16E-4) connected to a laptop computer. The acquisition software was developed with LabView. The signals are usually acquired at 50 ksample/s, i.e. with a 3 Hz square signal frequency and a 50% duty cycle, one scan acquisition consisting of 9000 data points requires 180 ms.

## 4 Quantum cascade laser characterization

### 4.1 Quasi-cw operation

We chose to operate the QC laser in a quasi-cw mode, as already done with cw QCLs at cryogenic temperatures [11]. In a pure cw mode, the heat dissipation produces a  $15\text{ }^{\circ}\text{C}$  temperature increase of the laser heat sink. Due to this effect, the laser threshold, which increases with the QCL heat-sink temperature, is almost equal to the maximum allowed current in the QCL structure. As a result, both the injection current and the QCL heat-sink temperature cannot be adjusted. Therefore, the QCL frequency cannot be tuned and the available output power is low.

To minimize thermal effects, quasi-continuous excitation consisting of injected square current signals in the 1–10 Hz frequency range, with a duty cycle of 5%–50%, were applied to the QCL. The current is applied to the QC laser for  $\sim 100\text{ ms}$  and then the laser is switched off for the same amount of time. The typical QCL current signal applied and the corresponding detected voltage are depicted in Fig. 2a and b. This mode of operation decreases the average injected current by a factor of two and the dissipated power by a factor of four, thus decreasing the laser threshold from 750 mA to 520 mA (the laser heat-sink temperature is lowered from  $-30\text{ }^{\circ}\text{C}$  to  $-45\text{ }^{\circ}\text{C}$ ). The QCL frequency now becomes tunable by adjusting the current level over a range of more than 200 mA. This operating method also intrinsically results in the tuning of the QCL frequency by self-heating of the laser-active zone. This effect is basically the same as the thermal chirp observed in intrapulse spectroscopy using pulsed QCLs [12, 13], but on the longer time scale permitted by the cw TEC QCL. The self-heating results in a decrease of the QCL output power

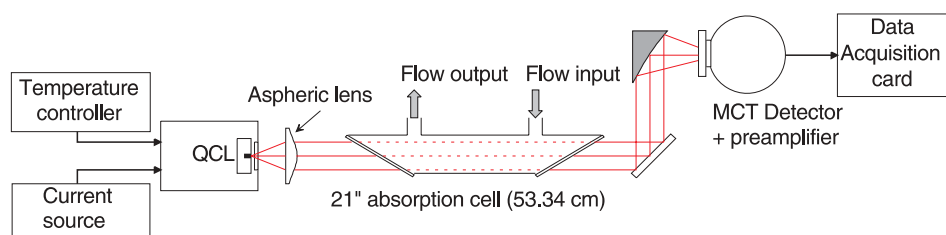
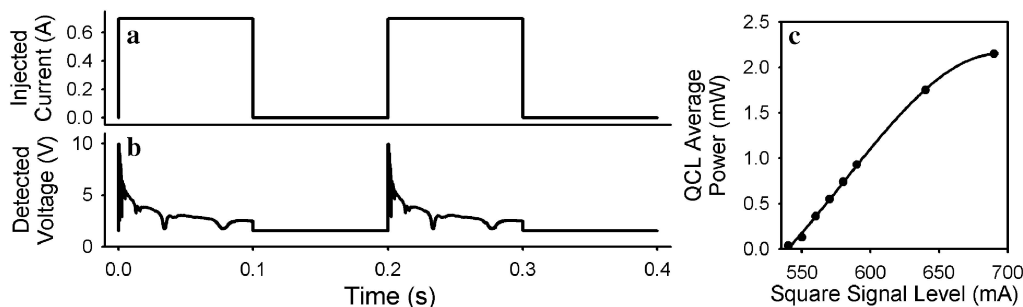


FIGURE 1 Layout of the QCL-based direct absorption spectroscopy setup



**FIGURE 2** Typical laser excitation signal involved in quasi-cw TEC QCL operation. **a** depicts the injected square current signal, **b** is the corresponding signal acquired, and **c** shows the average QCL optical power as a function of the injected square current signal level

(Fig. 2b), as well as frequency tuning. The absorption signal shown in Fig. 2b corresponds to when the gas cell was filled with SO<sub>2</sub> at a 5 Torr pressure (6.7 mbar). By operating the laser in a quasi-cw mode the available optical power increases to  $\sim 2$  mW. Figure 2c shows the average QCL optical power as a function of the amplitude of the injected current signal.

#### 4.2 Frequency calibration

The QCL frequency change that occurs because of self-heating was investigated to determine the frequency calibration of the QCL operating in a quasi-cw mode. An absolute frequency calibration was performed using a spectral identification of the experimental spectrum with the expected spectrum from the HITRAN 2000 spectral database. At the QCL laser wavelength used in this work, the density of spectral lines within the  $\nu_1$  band of SO<sub>2</sub> is high and the acquired experimental spectrum allows a non-ambiguous spectral recognition as shown in Fig. 3a. Using pure SO<sub>2</sub> at a 5 Torr

total pressure (6.7 mbar), a reliable calibration was performed and is presented in Fig. 3b. As depicted in Fig. 3c and d, the calibration was verified by inserting an etalon (consisting of two ZnSe wedge windows appropriately aligned) with a  $0.026\text{-cm}^{-1}$  free spectral range in the optical path. The total frequency coverage of one scan resolved by the detection system is  $\sim 0.5\text{ cm}^{-1}$ . The frequency can actually be scanned over several wavenumbers as reported in [12], but a ns acquisition system would be required to resolve the complete spectral scan. Our scans have a non-linear relationship between frequency and time and must be fitted. The best fitting function was found to be a logarithmic decay:

$$\sigma = \sigma_0 + a \ln(x - x_0), \quad (1)$$

where  $x$  denotes the data points.  $\sigma_0$ ,  $a < 0$ , and  $x_0$  are the fitting parameters whose values are given in the inset of Fig. 3b. The retrieved coefficients obtained either by SO<sub>2</sub> spectral recognition or using etalon fringes are close to each other. In par-

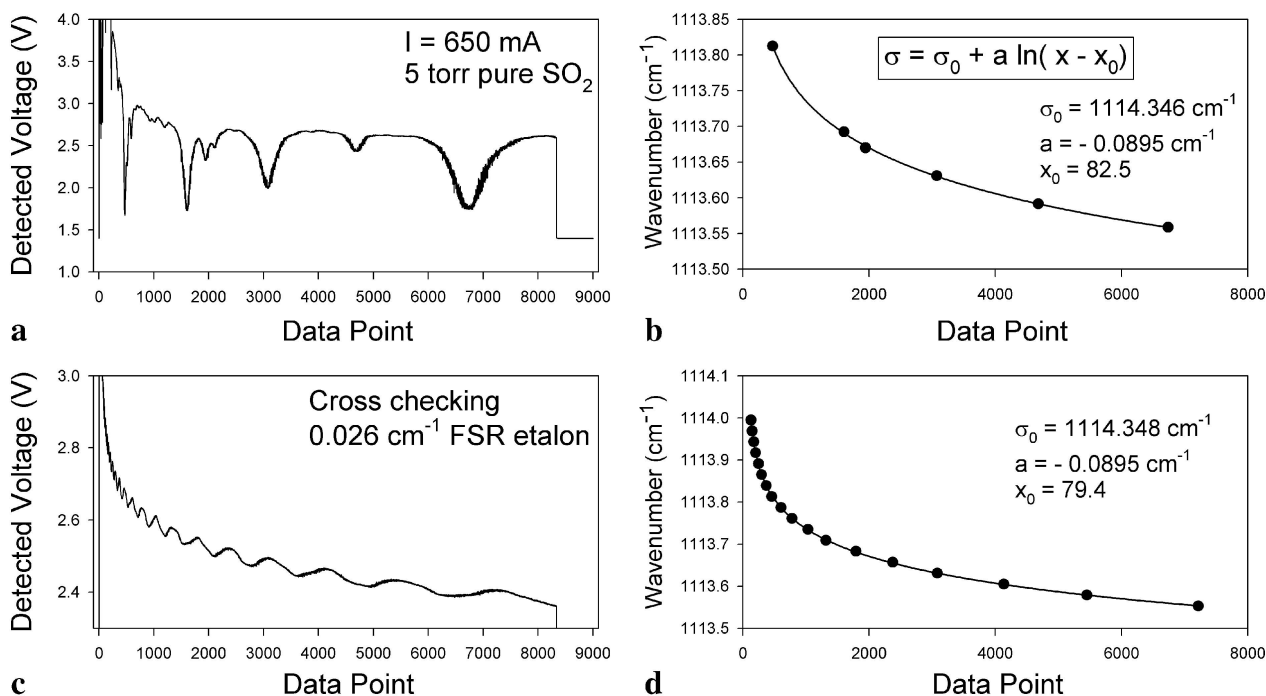


**FIGURE 3** QCL frequency calibration curves. **a** SO<sub>2</sub> spectra used for spectral recognition by a comparison with HITRAN 2000 data. **b** Related calibration curve where each point corresponds to the frequency of a SO<sub>2</sub> absorption line from (a). **c** Calibration with an etalon and **d** corresponding calibration curve

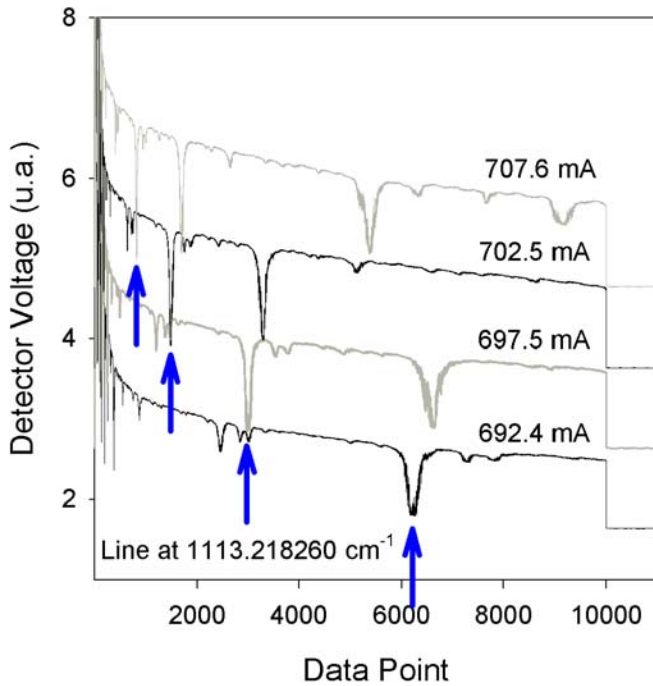


**FIGURE 4** Different  $\text{SO}_2$  absorption spectra for different current levels recorded for determining the effective current tuning rate of the 9.1- $\mu\text{m}$  QCL emission frequency

ticular, the most significant parameter  $a$  ( $\sigma_0$  and  $x_0$  are translation parameters) remains unchanged whatever the calibration technique. As a result of non-linear scanning in frequency, the density of experimental points is higher at the end of the scan than at the beginning, i.e. one has a higher density of experimental data points at low wavenumbers.

The laser is tunable from  $1115.8\text{ cm}^{-1}$  (square signal current level 520 mA, heat-sink temperature  $-41.2^\circ\text{C}$ ) to  $1111.8\text{ cm}^{-1}$  (700 mA and  $-26^\circ\text{C}$ ), which corresponds to a  $4\text{-cm}^{-1}$  tuning range. To determine an effective current tuning rate, several scans for different current levels were recorded. In Fig. 4, the arrow indicates the  $\text{SO}_2$  line at  $1113.218\text{ cm}^{-1}$ , showing the frequency shift that occurs due to variations of the current waveform level. The frequency tuning process in QCLs is caused by temperature effects. The drive current modifies the amount of heat dissipated in

the QC laser chip and consequently modifies its temperature. For a given data point of the scan, the effective current tuning rate  $\Delta\sigma/\Delta I$  was found to be  $-17.5\text{ cm}^{-1}/\text{A}$ , i.e.  $\Delta\nu/\Delta I = -525\text{ MHz/mA}$ . The effective current tuning rate is large compared to the typical tuning rate of a pulsed QCL in the same wavelength region, because of the much larger duty cycle in the quasi-cw operating mode.

### 4.3 QCL line-width study

As discussed in Sect. 1, the pulsed QCL spectrometer sensitivity and selectivity are affected by thermal chirp that degrades the laser line width [3]. With the intrapulse approach [12, 13], the effective line width depends only on the excitation pulse and a fast data-acquisition system is required. The line width of the laser in the quasi-cw-mode approach was investigated using an isolated  $\text{SO}_2$  line (at  $1114.174\text{ cm}^{-1}$ ).  $\text{SO}_2$  is a heavy molecule and consequently has a small Doppler line width ( $\Delta\nu_{\text{Dopp}} = 53\text{ MHz}$ ). The line width of the absorption feature was measured for different pure  $\text{SO}_2$  pressure levels in the cell including pressures at which pressure broadening is well below the Doppler limit. The measurements are summarized in Fig. 5a and 5b. At pressures above 8 Torr (10.7 mbar) collisional broadening prevails and the QC laser line-width contribution remains insignificant. The experimental and theoretical points of Fig. 5b coincide. At low pressure, the influence of the laser line width starts to appear and becomes obvious for pressures below 0.2 Torr (0.3 mbar), where the Doppler limit is reached. At pressures below 0.2 Torr, the  $\text{SO}_2$  absorption line exhibits an observed full width at half maximum (FWHM)  $\Delta\nu_{\text{obs}}$  of  $72 \pm 7\text{ MHz}$ . If we assume a Gaussian line shape with a FWHM  $\Delta\nu_{\text{Las}}$  for the laser spectrum, a convolution yields

$$\Delta\nu_{\text{obs}}^2 = \Delta\nu_{\text{Dop}}^2 + \Delta\nu_{\text{Las}}^2. \quad (2)$$

From (2) we obtain that the QCL line width is  $47 \pm 11\text{ MHz}$ . This line-width value is directly related to the current-source noise. The fluctuations of the current source were measured for a 700-mA output and, within the current-source bandwidth, the current standard deviation is  $\sigma_I = 50\text{ }\mu\text{A}$ . According to the effective tuning rate as determined above

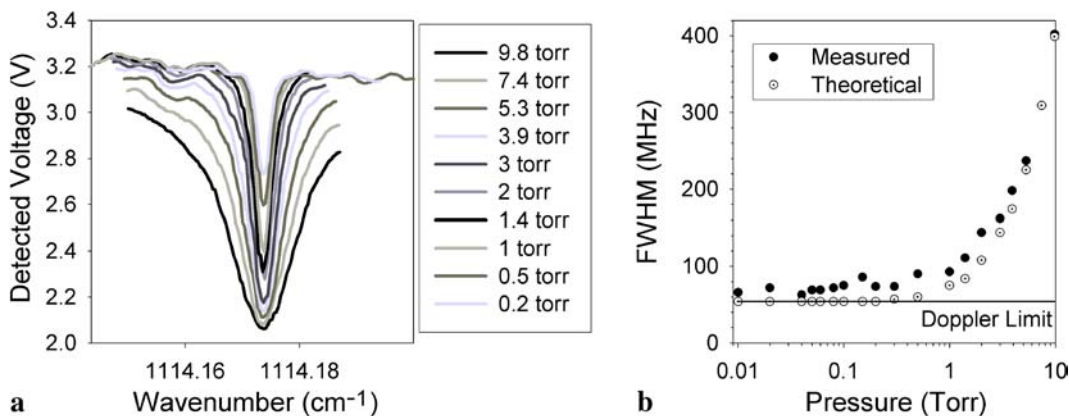


**FIGURE 5** a Line shape for different pressures of a  $\text{SO}_2$  absorption line. b Corresponding FWHM measurements

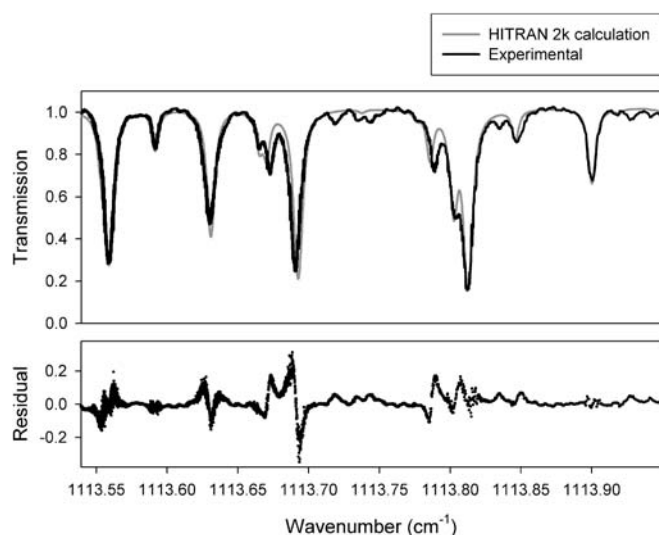


**FIGURE 6** A single  $0.5\text{-cm}^{-1}$  scan of a  $\text{SO}_2$  spectrum recorded in a quasi-cw mode (3 Hz, 50% duty cycle). The experimental spectrum is compared to a simulated spectrum based on HITRAN data

(525 MHz/mA), the FWHM of the QC laser is given by

$$\text{FWHM} \approx 2 \sigma_I \frac{\Delta \nu}{\Delta I}. \quad (3)$$

Equation (3) yields a FWHM of 52.5 MHz, which is consistent with the  $47 \pm 11$  MHz value determined experimentally.

This QCL line-width value is close to the one observed in the pure cw mode at cryogenic temperatures by Sharpe et al. [14] ( $\sim 40$  MHz) but still high compared to the  $\sim 1$  MHz achievable by reducing the current-source noise [15]. However, such a QCL line width is at least five times below the one observed in pulsed mode operation and insignificant if performing gas-concentration measurements at reduced pressures of  $\sim 100$  Torr (133.3 mbar). This line width represents an effective improvement compared to the line width of a pulsed QC laser, which is a key parameter in isotopic studies where sensor selectivity is required. This laser line width can be further improved by the development of a low-noise current source.

## 5 Direct absorption spectroscopy

Direct spectroscopic  $\text{SO}_2$  absorption measurements were performed at a 5 Torr cell pressure (6.7 mbar). A laser scan was made with the following parameters: acquisition frequency 50 kS/s, duty cycle 50%, 9000 points per scan, square excitation signal level 650 mA, and a laser heat-sink temperature of  $-40^\circ\text{C}$ . The signal from the detector is shown in Fig. 3a. The scan is  $\sim 10$  ms longer than the half period of the excitation signal in order to measure the detector voltage while the laser is turned off. The detector provides a voltage offset, which has to be removed. The signal is then processed according to the following steps: absolute frequency calibration using (1), a polynomial baseline correction, and a comparison of the experimental spectrum with a calculated spectrum based on HITRAN 2000 data and on the Olivero and Longbothum line-shape approximation for a Voigt profile [16]. The results are presented in

Fig. 6. The weak  $\text{SO}_2$  lines that appear in the experimental spectrum are not included in the HITRAN 2000 database. It can also be seen that slight frequency shifts of some of the weak lines are observable that indicate a discrepancy in the frequency-calibration procedure. The laser line width might also have a small effect at 5 Torr pressure and not be insignificant as assumed. Overall, the fit of the experimental spectrum is in good agreement with the calculated spectrum.

The sensor was then applied to the detection and quantification of trace-gas species. To study the minimum detection sensitivity achievable by tunable cw TEC QCL absorption spectroscopy, spectra of a calibrated  $\text{NH}_3 : \text{N}_2$  mixture were acquired. The calibrated ammonia concentration was certified to be  $1038 \pm 21$  ppm by the gas provider (Matheson Trigas). The calibration measurements were performed using a flow configuration to limit  $\text{NH}_3$  adsorption-desorption in the gas system [17], which is important with the stainless steel cell used in these tests. The pressure is kept constant by a pressure controller set to 99.4 Torr (132.5 mbar).

For this particular experiment, the laser was operated at 2 Hz with a 5% duty cycle to narrow the frequency-scan range around the spectral feature of interest. The square signal level was 730 mA, the QCL heat-sink temperature was  $-46^\circ\text{C}$ , and 5000 points were acquired at a 200-kS/s rate. According to HITRAN, the target line is located at  $1112.949\text{ cm}^{-1}$  and the transition intensity is  $2.429 \times 10^{-20}\text{ cm}^{-1}/\text{molec. cm}^{-2}$ , which is  $\sim 10$  times higher than the  $\text{NH}_3$  intensities reported in the near-infrared region [18]. To obtain the spectrum presented in Fig. 7, the process is identical to the one described above for  $\text{SO}_2$  spectroscopy: the recorded raw data are frequency recalibrated and a polynomial baseline correction is applied. The experimental spectrum is fitted by a routine developed with LabView and based on the Levenberg-Marquardt iterative fitting method. Using HITRAN, a theoretical spectrum is calculated. Four parameters are left free to be fitted: the  $\text{NH}_3$  concentration, a frequency offset (to correct potential errors of the calibration procedure), the baseline offset, and the baseline slope (to correct potential errors of the baseline-removal procedure). The concentration retrieved by this procedure was found to be  $1163 \pm 11$  ppm. This value represents a 12% overestimate compared to the gas-provider certification. Taking the gas-mixture calibration as a reference, either a  $\text{NH}_3$  desorption process by the cell or the accuracy of the absorption line strength given by HITRAN could be responsible for this discrepancy. The HITRAN data is believed to be responsible for the discrepancy, as the gas system was operated in a flow configuration for a time sufficiently long to let the  $\text{NH}_3$  concentration reach equilibrium. From the residual spectrum shown in the bottom part of Fig. 7, the standard deviation was calculated and used to extrapolate the  $1\sigma$  noise-equivalent sensitivity (NES). The residual spectrum exhibits higher values at shorter wavelengths because of the laser amplitude modulation associated with the scan. The standard deviation is  $2.8 \times 10^{-3}$ . This corresponds to a fractional absorption of 36 ppm of  $\text{NH}_3$  for the 53.34-cm absorption cell used in this study. It corresponds to a NES of 18 ppm for 1 m of absorption for a single-frequency scan in a 25-ms data-acquisition time. For comparison, Claps et al. [19] reported a 0.23 ppm

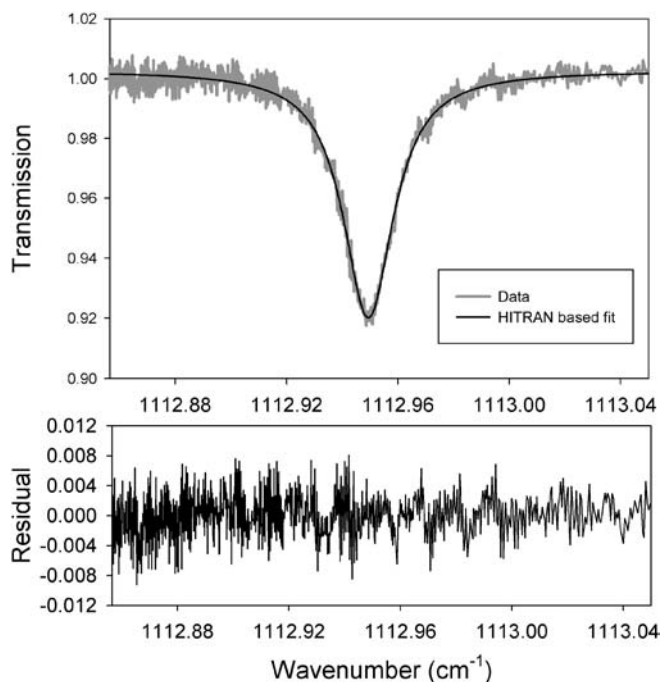


**FIGURE 7** Direct absorption spectrum of a calibrated  $\text{NH}_3 : \text{N}_2$  mixture with a 1038 ppm  $\text{NH}_3$  concentration is represented by the grey data. The black line spectrum is a fit based on the Levenberg–Marquardt routine. The fit yields a  $\text{NH}_3$  concentration of 1163 ppm

NES for a 36-m multipass cell and 500 scans averaged by using near-infrared absorption spectroscopy. This value for the NES corresponds to 185 ppm for 1 m of absorption for a single scan assuming white noise. Hence, we measure a NES of one order of magnitude better in the mid infrared due to the higher  $\text{NH}_3$  line strength of the transition that was used. Kosterev et al. reported 0.3 ppm for a 1-m absorption path with a 10-s data-acquisition time using a pulsed 10- $\mu\text{m}$  quantum cascade laser [20]. This corresponds to a NES of 6 ppm per m of absorption for a 25-ms acquisition time.

The main sensitivity limitation of the gas sensor was found to arise from residual etalon fringes. These fringes can exhibit a contrast of up to 2%. However, by means of optical adjustment these fringes can be partially removed as shown in the residual trace of Fig. 7. For these  $\text{NH}_3$  measurements, some excess intensity noise was also observed because the laser operating point required for accessing the optimum  $\text{NH}_3$  line was close to a potential mode-hop region.

## 6 Wavelength-modulation spectroscopy

Wavelength-modulation spectroscopy (WMS) is a technique widely used for sensitive absorption spectroscopy with cw tunable lasers [21]. The technique was first applied to pulsed QCLs by Namjou et al. to monitor  $\text{N}_2\text{O}$  [22]. Theoretically, an improvement of one order of magnitude in the sensitivity is expected compared to direct absorption spectroscopy [23] due to a higher signal to noise ratio (laser noise is smaller at kHz frequencies) and due to a reduced sensitivity to the baseline. The cw TEC QCL based gas sensor benefits from the implementation of WMS. For this study, a si-

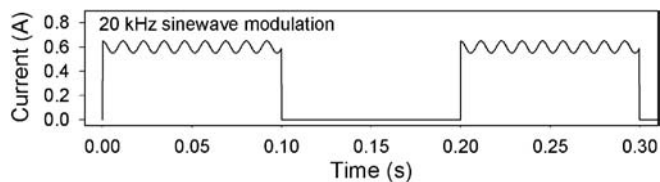


**FIGURE 8** Schematic of the current excitation signal applied to the QCL to perform quasi-cw wavelength-modulation spectroscopy. The sinusoidal modulation amplitude and frequency depicted here are not shown to scale for clarity

nusoidal waveform was superimposed on to the square signal as described previously (see Fig. 2), in order to generate the excitation signal shown in Fig. 8.

The square signal and the sinusoidal waveform have to be synchronized to ensure a constant phase relation between them and to avoid any arbitrary signal fluctuation after the demodulation process. The wavelength-modulation frequency must be a multiple of the quasi-cw signal frequency and the two waveform generators providing these signals (Analogic model 2030 and SRS model DS345) must operate with the same time base (a 10-MHz time-base signal). For the quasi-cw signal the same settings already described for the direct absorption spectroscopy experiment were used. The sinusoidal signal is set to 20 kHz. The modulation amplitude was found to be optimum at 4.2 mA peak to peak. This modulation depth corresponds to 2.2 GHz, which is approximately three times the full width at half maximum of the  $\text{NH}_3$  line at 99.4 Torr. Second-harmonic detection was implemented by means of a lock-in amplifier (SRS model SR830). The demodulated signal obtained after wavelength calibration is depicted in Fig. 9. The asymmetric shape appearing in Fig. 9 is believed to be due to the important and strongly non-linear variation of the laser power during the scan.

The lock-in amplifier sensitivity is set to 5 mV and its time constant to 30  $\mu\text{s}$ . By considering the noise on the detected signal of the  $\text{NH}_3$  spectral absorption feature, the  $1\sigma$  NES of the sensor can be determined. The standard deviation of

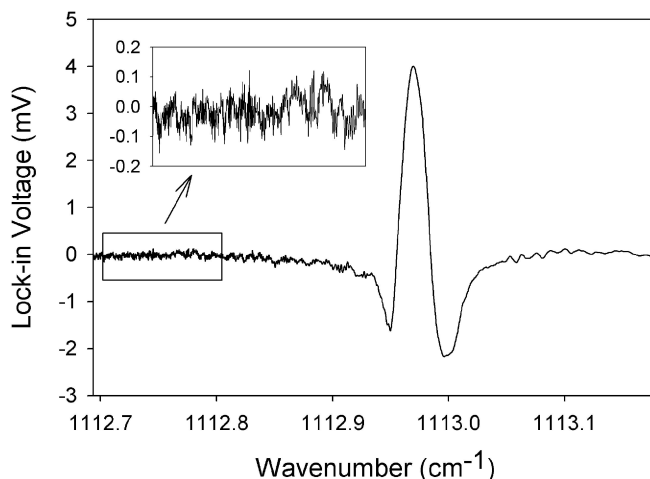


**FIGURE 9** Absorption signal of 1038 ppm of  $\text{NH}_3$  diluted in nitrogen obtained by wavelength-modulation spectroscopy with detection at the second harmonic. The lock-in amplifier time constant is 30  $\mu\text{s}$

the lock-in amplifier voltage is 0.045 mV. This corresponds to a  $\text{NH}_3$  concentration of 12 ppm, i.e. 82 ppb  $\text{m Hz}^{-1/2}$  sensitivity scaled to the absorption path length and the detection bandwidth set by the lock-in amplifier time constant. In term of the absorption coefficient this figure of merit becomes  $2 \times 10^{-7} \text{ cm}^{-1} \text{ Hz}^{-1/2}$ . A factor of three was gained for the sensitivity of the gas sensor by applying WMS with second-harmonic detection. A detection sensitivity comparable to the one reported in [20] was achieved but with a considerably less complicated setup involving no high-speed electronics and synchronization. This technique is commonly limited by the noise originating from the residual amplitude modulation and, in this particular case, by the laser excess noise already mentioned.

## 7 Conclusion

This study demonstrated the feasibility and performance level of gas-sensing applications using recently developed cw TEC DFB quantum cascade lasers, which are applicable to the development of quasi-room-temperature mid-infrared optical sensors with no need of expensive nanosecond electronics and cryogenic cooling. A quasi-cw mode resulting in a larger QCL frequency coverage was found to be the most efficient approach for gas sensing, with a reduced laser line width compared to pulsed QCL operation. The QCL-based sensor demonstration was carried out based on direct absorption spectroscopy of  $\text{SO}_2$  and  $\text{NH}_3$ . The optimum sensitivity obtained to date using wavelength-modulation spectroscopy with detection at the second harmonic was achieved with the reported quasi-cw 9- $\mu\text{m}$  TEC DFB QCL based gas sensor. The normalized noise-equivalent sensitivity for ammonia was found to be 82 ppb  $\text{Hz}^{-1/2}$  for a 1-m path length.

**ACKNOWLEDGEMENTS** The authors wish to thank R.F. Curl for his most helpful comments and suggestions. The authors also gratefully acknowledge financial support from the National Aeronautics and Space Administration, the Texas Advanced Technology Program, the Robert Welch Foundation, and the Office of Naval Research via a sub-award from Texas A&M University. T. Aellen, M. Beck, S. Blaser and J. Faist would like to acknowledge financial support from the National Centre of Competence in Research "Quantum Photonics".

## REFERENCES

- 1 A.A. Kosterev, F.K. Tittel: IEEE J. Quantum Electron. **QE-38**, 582 (2002)
- 2 D.M. Sonnenfroh, W.T. Rawlins, M.G. Allen, C.G. Gmachl, F. Capasso, A.L. Hutchinson, D.L. Sivco, J.N. Baillargeon, A.Y. Cho: Appl. Opt. **40**, 812 (2001)
- 3 D.D. Nelson, J.H. Shorter, J.B. McManus, M.S. Zahniser: Appl. Phys. B **75**, 343 (2002)
- 4 D. Weidmann, A.A. Kosterev, C. Roller, R.F. Curl, M.P. Fraser, F.K. Tittel: Appl. Opt. **43**, 3329 (2004)
- 5 M. Beck, D. Hofstetter, T. Aellen, J. Faist, U. Oesterle, M. Illegems, E. Gini, H. Melchior: Science **295**, 301 (2002)
- 6 A. Evans, J.S. Yu, J. David, L. Doris, K. Mi, S. Slivken, M. Razeghi: Appl. Phys. Lett. **84**, 314 (2004)
- 7 T. Aellen, S. Blaser, M. Beck, D. Hofstetter, J. Faist, E. Gini: Appl. Phys. Lett. **83**, 1929 (2003)
- 8 S. Blaser, L. Hvozdar, Y. Bonetti, A. Muller, M. Giovannini, J. Faist: in *CLEO 2004, San Francisco, CA, 16–21 May 2004*, postdeadline paper CPDB6
- 9 L.S. Rothman, A. Barbe, D.C. Benner, L.R. Brown, C. Camy-Peyret, M.R. Carleer, K. Chance, C. Clerbaux, V. Dana, V.M. Devi, A. Fayt, J.-M. Flaud, R.R. Gamache, A. Goldman, D. Jacquemart, K.W. Jucks, W.J. Lafferty, J.-Y. Mandin, S.T. Massie, V. Nemtchinov, D.A. Newham, A. Perrin, C.P. Rinsland, J. Schroeder, K.M. Smith, M.A.H. Smith, K. Tang, R.A. Toth, J. Vander Auwera, P. Varanasi, K. Yoshino: J. Quantum Spectrosc. Radiat. Transfer **82**, 5 (2003)
- 10 J.H. Seinfeld, S.N. Pandis: *Atmospheric Chemistry and Physics* (Wiley, New York 1997) Chap. 2
- 11 A.A. Kosterev, R.F. Curl, F.K. Tittel, C. Gmachl, F. Capasso, D.L. Sivco, J.N. Baillargeon, A.L. Hutchinson, A.Y. Cho: Appl. Opt. **39**, 4425 (2000)
- 12 E. Normand, M. McCulloch, G. Duxbury, N. Langford: Opt. Lett. **28**, 16 (2003)
- 13 T. Beyer, M. Braun, A. Lambrecht: J. Appl. Phys. **93**, 3158 (2003)
- 14 S.W. Sharpe, J.F. Kelly, J.S. Hartman, C. Gmachl, F. Capasso, D.L. Sivco, J.N. Baillargeon, A.Y. Cho: Opt. Lett. **23**, 1396 (1998)
- 15 D. Weidmann, L. Joly, V. Parpillon, D. Courtois, Y. Bonetti, T. Aellen, M. Beck, J. Faist, D. Hofstetter: Opt. Lett. **28**, 704 (2003)
- 16 J.J. Olivero, R.L. Longbothum: J. Quantum Spectrosc. Radiat. Transfer **17**, 233 (1977)
- 17 A. Schmohl, A. Miklos, P. Hess: Appl. Opt. **40**, 2571 (2001)
- 18 M.E. Webber, D.S. Baer, R.K. Hanson: Appl. Opt. **40**, 2031 (2001)
- 19 R. Claps, F.V. Englich, D.P. Leleux, D. Richter, F.K. Tittel: Appl. Opt. **40**, 4387 (2001)
- 20 A.A. Kosterev, R.F. Curl, F.K. Tittel, R. Köhler, C. Gmachl, F. Capasso, D.L. Sivco, A.Y. Cho: Appl. Opt. **41**, 573 (2002)
- 21 J.T.C. Liu, J.B. Jeffries, R.K. Hanson: Appl. Phys. B **78**, 503 (2004)
- 22 K. Namjou, S. Cai, E.A. Whittaker, J. Faist, C. Gmachl, F. Capasso, D.L. Sivco, A.Y. Cho: Opt. Lett. **23**, 219 (1998)
- 23 J.A. Silver: Appl. Opt. **31**, 6 (1992)